NASA TECHNICAL NOTE

NASA TN D-2213

NASA TN D-2213

HEAT TRANSFER FOR LAMINAR SLIP FLOW OF A RAREFIED GAS IN A PARALLEL-PLATE CHANNEL OR A CIRCULAR TUBE WITH UNIFORM WALL TEMPERATURE

by Robert M. Inman

Lewis Research Center
Cleveland, Ohio

NATIONAL AERONAUTICS AND SPACE ADMINISTRATION • WASHINGTON, D. C. • NOVEMBER 1964

HEAT TRANSFER FOR LAMINAR SLIP FLOW OF A RAREFIED GAS IN A PARALLEL-PLATE CHANNEL OR A CIRCULAR TUBE WITH UNIFORM WALL TEMPERATURE

By Robert M. Inman

Lewis Research Center
Cleveland, Ohio

NATIONAL AERONAUTICS AND SPACE ADMINISTRATION

For sale by the Office of Technical Services, Department of Commerce,
Washington, D.C. 20230 -- Price $1.00

HEAT TRANSFER FOR LAMINAR SLIP FLOW OF A RAREFIED GAS IN A PARALLEL-PLATE CHANNEL OR A CIRCULAR TUBE WITH UNIFORM WALL TEMPERATURE

by Robert M. Inman

Lewis Research Center

SUMMARY

An analysis has been made to determine the effects of low-density phenomena on the heat-transfer characteristics for laminar flow in a parallel-plate channel or in a circular tube with uniform wall temperature. Consideration is given to the slip-flow regime wherein the major rarefaction effects are displayed as velocity and temperature jumps at the conduit walls. The results apply along the entire length of the conduit. The solutions contain a series expansion, and analytical expressions for the complete set of eigenvalues and eigenfunctions for the problems are presented. The results give the temperature of the gas adjacent to the wall, the wall heat flux, and the Nusselt numbers for the conduits for various values of the rarefaction parameters.

INTRODUCTION

In recent years considerable interest has developed in the study of the heat-transfer characteristics of rarefied gases flowing inside conduits. This interest in the rarefied gas mode of heat transfer has been spurred by the advent of high-altitude flight and by the low-density environment that is being encountered with increasing frequency in present day technology. Under the conditions of high-altitude flight, for example, the gas flow inside a conduit may be sufficiently rarefied so that the appropriate mean free path becomes too large for the use of the usual continuum-transfer equations but not large enough for free-molecule or transition concepts to apply.

In this regime of slight gas rarefaction, termed the slip-flow regime, which is the gas regime considered in this investigation, the gas adjacent to a solid surface no longer assumes the velocity and temperature of the surface. Instead, the gas slips along the surface, and, in addition, there is a jump in temperature between the surface and the adjacent gas. The effects of these rarefaction phenomena on the heat-transfer characteristics for laminar flow inside ducts and tubes are of practical interest to the engineer concerned with the design and analysis of compact heat-exchange equipment for high-altitude-flight or low-density-environment applications.

Two geometries that are commonly encountered in practice are selected for analysis, the parallel-plate channel and the circular tube. A uniform-wall-temperature boundary condition is considered. There are many practical situations that require the design and analysis of apparatus for heating or cooling a gas flowing through a conduit with the conduit walls maintained at a constant temperature, for example, flow through compact heat exchangers where one fluid is at constant temperature because of a change of phase or flow through heat exchangers where the capacity rate of the gas is so much lower than that of the other fluid that an essentially constant wall temperature is attained.

The heat-transfer characteristics of slightly rarefied gases flowing inside a parallel-plate channel or inside a circular tube have been considered in three previous papers. In reference 1 the effects of slight rarefaction on the fully developed heat-transfer characteristics for laminar flow in tubes were studied analytically. The analysis was carried out for both uniform wall heat flux and uniform wall temperature.

In reference 2 the effects of second-order terms on the velocity and temperature jumps at a wall were obtained by a physical derivation, and the results were used to determine the fully developed heat transfer in a tube with uniform wall heat flux.

The results of the foregoing analyses are limited to the region where the temperature distribution is fully developed, and, hence, the solutions do not apply in the thermal entrance region. Reference 3 contains an analytical study of the effects of slight gas rarefaction on the heat-transfer characteristics for fully developed laminar flow in a parallel-plate channel or in a circular tube with a uniform wall heat flux. The results obtained for both geometries are applicable along the entire length of the conduit, that is, in the thermal entrance region as well as far downstream. The solutions contain a series expansion that arises in connection with the entrance-region heat-transfer analysis, and analytical expressions for the eigenvalues and constants are presented. Numerical solutions of these important quantities are also obtained through the use of an electronic (IBM 7094) computer, and comparisons are made that show very good agreement between the two methods of computation.

The present investigation is concerned with laminar flow of an incompressible, slightly rarefied gas in a parallel-plate channel or in a circular tube with uniform wall temperature. For the uniform wall-temperature problem, a knowledge of the eigenfunctions and eigenvalues is not only necessary in the entrance region but also in the fully developed region (at least the first eigenvalue is necessary in the fully developed region). The flow between the parallel plates or in the tube is assumed to be fully developed. This implies that a hydrodynamic entrance length is present that allows the gas to establish a fully developed velocity distribution before reaching the heated section of the conduit. In addition, the assumption implies that the thermal creep velocity, which is an additional velocity induced when a gas adjacent to a surface encounters a temperature gradient along the surface (ref. 4), can be neglected. The solutions without the inclusion of thermal creep will then represent the zeroth-order solutions with regard to this effect.

This assumption, however, allows the velocity field to be determined independently of the temperature (whereas the temperature field is a function of the velocity), and it is believed that the understanding gained will lead to more precise and more extensive study.

The parallel-plate channel is considered first, and two cases of practical interest are examined: a step change in wall temperature at both plates and a step change in wall temperature at the upper plate only, while the lower wall is insulated. The circular tube configuration is then analyzed for a step in wall temperature. The results obtained for both geometries are applicable along the entire length of the passages.

Before the energy equation can be solved, the gas velocity distribution must be known. This has been investigated in reference 3 for the parallel-plate channel and in references 1 and 4 for the circular tube, and the results will be used in the present study.

With the velocity distributions known, the energy equation can be considered. The solutions involve series expansions, and analytical expressions will be derived for the eigenvalues and constants as functions of the gas rarefaction parameters.

RAREFIED GAS FLOW IN A PARALLEL-PLATE CHANNEL

WITH STEP CHANGE IN WALL TEMPERATURE

This portion of the analysis is concerned with fully developed laminar flow of a slightly rarefied gas between parallel plates as illustrated in figure 1. For $x < 0$, the plates and the gas are assumed to be isothermal at temperature t_e; whereas for $x \geq 0$, the wall (both the upper and the lower, or else the upper only with the lower wall insulated) temperature is step-changed to a new value t_w. (All symbols are defined in appendix A.)

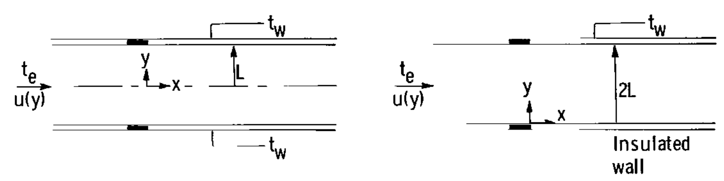

(a) Symmetry number, 2. (b) Symmetry number, 1.

Figure 1. - Physical model and coordinate system for parallel-plate channel.

Energy Equation

The energy equation for incompressible flow in a parallel-plate channel can be written as

$$u \frac{\partial t}{\partial x} = \alpha \frac{\partial^2 t}{\partial y^2} \tag{1}$$

To obtain the equation in this form, viscous dissipation and axial heat conduction are neglected compared with heat conduction in the transverse direction. It is convenient to place the plane $y = 0$ at the plane of symmetry, that is, at the middle plane of the channel in case of a step change in temperature at both walls (fig. 1(a)) and at the lower wall in case of a step in temperature at the upper wall only (fig. 1(b)).

Both cases can be included in the following development by defining a symmetry number σ, which is also the number of walls step-changed in temperature; that is, $\sigma = 2$ if both wall temperatures are changed, and $\sigma = 1$ if only the upper wall temperature is changed, the lower wall being insulated.

It is also convenient to rewrite equation (1) in terms of dimensionless variables; then equation (1) is given as

$$f(\eta) \frac{\partial T}{\partial \zeta} = \frac{\partial^2 T}{\partial \eta^2} \tag{2}$$

The dimensionless velocity distribution $f(\eta)$ is obtained from reference 4 and is different for each value of σ:

$$\left.\begin{aligned} f(\eta) &= \frac{\frac{3}{2}(1 - \eta^2 + 4\lambda)}{1 + 6\lambda} \qquad \text{for} \quad \sigma = 2 \\ f(\eta) &= \frac{6(\eta - \eta^2 + \lambda)}{1 + 6\lambda} \qquad \text{for} \quad \sigma = 1 \end{aligned}\right\} \tag{3}$$

where $\lambda \equiv \xi_u/2L$. The velocity-slip coefficient ξ_u has been related by Maxwell to other properties of the system by the expression (ref. 5)

$$\xi_u = \frac{2 - g}{g} l \tag{4}$$

where g is the specular reflection coefficient and l is the mean free path

$$l = \sqrt{\frac{\pi}{2}} \frac{\mu \sqrt{R_g t}}{p} \tag{5}$$

The relation between the average velocity and the slip velocity may be obtained from equation (3) by setting $\eta = 1$

$$\frac{u_s}{\bar{u}} = f(1) = \frac{6\lambda}{1 + 6\lambda} \qquad \text{for} \quad \sigma = 2,1 \tag{6}$$

The dimensionless temperature T is defined so that at the entrance of the heated section the value of T is unity.

Solution

Equation (2) is to be solved subject to the boundary conditions

$$
\left.\begin{aligned}
&T = 1 \qquad \text{at} \quad \zeta = 0 \quad \text{for all} \quad \eta \text{ (entrance condition)} \\
&\frac{\partial T}{\partial \eta} = 0 \qquad \text{at} \quad \eta = 0 \text{ (symmetry)}
\end{aligned}\right\} \tag{7}
$$

Another effect of the gas rarefaction enters through the boundary condition at the channel wall, which permits a jump between the wall temperature t_w and the adjacent gas temperature t_g (ref. 5)

$$
t_g - t_w = -\sigma \frac{\xi_t}{2L} \left(\frac{\partial t}{\partial \eta}\right)_{\eta=1} \qquad \text{for} \quad \zeta > 0 \tag{8}
$$

where ξ_t denotes a temperature-jump coefficient, related to other properties of the system by the expression

$$
\xi_t = \frac{2 - a}{a} \frac{2\gamma}{\gamma + 1} \frac{l}{Pr} \tag{9}
$$

The solution of equation (2), which will satisfy conditions (7) and (8), can be found by using a product solution that leads to a separation of variables. Then the solution for T can be written as

$$
T = \frac{t - t_w}{t_e - t_w} = \sum_{n=0}^{\infty} b_n Y_n(\eta) \exp(-\beta_n \zeta) \tag{10}
$$

where the Y_n and β_n are the eigenfunctions and eigenvalues of the Sturm-Liouville problem

$$
\frac{d^2 Y_n}{d\eta^2} + \beta_n f(\eta) Y = 0 \qquad \text{for} \quad \sigma = 2,1 \tag{11a}
$$

with the boundary conditions

$$
\left.\begin{aligned}
&\frac{dY_n}{d\eta} = 0 \qquad \text{at} \quad \eta = 0 \\
&Y_n(1) = -\sigma \frac{\xi_t}{2L} \left(\frac{dY_n}{d\eta}\right)_{\eta=1}
\end{aligned}\right\} \tag{11b}
$$

The solution of equation (11a) will be taken up shortly.

The coefficients b_n also remain to be determined. These are evaluated to satisfy the condition at the entrance of the channel ($\zeta = 0$)

$$1 = \sum_{n=0}^{\infty} b_n Y_n(\eta) \tag{12}$$

Using the properties of the Sturm-Liouville system results in

$$b_n = \frac{\int_0^1 f(\eta) Y_n(\eta) d\eta}{\int_0^1 f(\eta) Y_n^2(\eta) d\eta} \qquad \text{for} \quad \sigma = 2,1 \tag{13a}$$

As shown in detail in appendix B, the integral appearing in the numerator may be written as

$$\int_0^1 f(\eta) Y_n(\eta) d\eta = -\frac{1}{\beta_n} \left(\frac{dY_n}{d\eta}\right)_{\eta=1} \tag{13b}$$

whereas the denominator of equation (13a) becomes

$$\int_0^1 f(\eta) Y_n^2(\eta) d\eta = \left(\frac{\partial Y}{\partial \beta} + \sigma \frac{\xi_t}{2L} \frac{\partial^2 Y}{\partial \eta \, \partial \beta}\right)_{\substack{\eta=1 \\ \beta=\beta_n}} \left(\frac{dY_n}{d\eta}\right)_{\eta=1} \tag{13c}$$

Then the series coefficients are

$$b_n = -\frac{1}{\beta_n \left(\frac{\partial Y}{\partial \beta} + \sigma \frac{\xi_t}{2L} \frac{\partial^2 Y}{\partial \eta \, \partial \beta}\right)_{\substack{\eta=1 \\ \beta=\beta_n}}} \qquad \text{for} \quad \sigma = 2,1 \tag{14}$$

This result implies that, once the eigenfunctions Y_n are known, the coefficients b_n of equation (10) may be calculated. Thus, it is apparent that a knowledge of the eigenvalues and the eigenfunctions of equation (11a) is essential to the temperature solution (eq. (10)). The possibility of determining these quantities analytically is one of the interesting aspects of the problem. The functions $Y_n(\eta)$ and the corresponding eigenvalues β_n are as yet undetermined. Before a calculation of these quantities is undertaken, however, the analysis will be extended to the formulation of several quantities of engineering interest.

From the temperature distribution (eq. (10)), several quantities of engineering interest can be determined: the axial variation of the gas temperature adjacent to the wall, the wall heat-flux variation along the channel length required to maintain the wall temperature constant, and the local Nusselt number variation. The axial variation of the gas temperature adjacent to the wall is obtained from equation (10) by setting $\eta = 1$ therein. In the absence of a temperature jump ($\xi_t = 0$), it is apparent, either from equation (8) or from the second part of equation (11b), that t_g = constant = t_w. With a temperature-jump effect, however, $t_g \neq t_w$. The heat flux at the wall can be evaluated from Fourier's law

$$q = \kappa\left(\frac{\partial t}{\partial y}\right)_{y=2L/\sigma} = \kappa(t_e - t_w)\,\frac{\sigma}{2L}\left(\frac{\partial T}{\partial \eta}\right)_{\eta=1} \tag{15}$$

where q is defined as the heat added at the wall. Applying this to equation (10) gives the result for the wall heat flux as a function of position along the channel:

$$q\,\frac{\frac{2L}{\sigma}}{\kappa(t_w - t_e)} = -\sum_{n=0}^{\infty} b_n\left(\frac{dY_n}{d\eta}\right)_{\eta=1}\exp(-\beta_n\zeta) \tag{16}$$

The Nusselt modulus may be defined by referring either to the hydraulic diameter D_H, equal to $4L$, or to a thermal diameter D_T, which depends on the area of the heating surface and in the present case is equal to $8L/\sigma$ (ref. 6). The latter definition will be adopted here, so that

$$Nu = \frac{hD_T}{\kappa} = \frac{\frac{2L}{\sigma}\,4q}{\kappa(t_w - t_b)} \tag{17}$$

Substituting q from equation (16), the Nusselt modulus may be written as

$$Nu = -4\sum_{n=0}^{\infty}\frac{t_w - t_e}{t_w - t_b}\,b_n\left(\frac{dY_n}{d\eta}\right)_{\eta=1}\exp(-\beta_n\zeta) \tag{18}$$

To put this in a more useful form, it is necessary to develop an expression for $(t_w - t_e)/(t_w - t_b)$. To do this, it is necessary to know the bulk temperature T_b, which may be found from

$$T_b = \frac{t_w - t_b}{t_w - t_e} = \frac{\int_0^1 uT\,d\eta}{\int_0^1 u\,d\eta} \tag{19}$$

Since $\int_0^1 u\, d\eta = \bar{u}$,

$$T_b = \int_0^1 Tf(\eta)d\eta \tag{20}$$

By introducing the temperature distribution (eq. (10)) into the bulk temperature (eq. (20)), the following is obtained:

$$\frac{t_w - t_b}{t_w - t_e} = \sum_{n=0}^{\infty} b_n \exp(-\beta_n\zeta) \int_0^1 f(\eta)Y_n(\eta)d\eta \tag{21}$$

The integration has been carried out in equation (B2) with the result

$$\int_0^1 f(\eta)Y_n(\eta)d\eta = -\frac{1}{\beta_n}\left(\frac{dY_n}{d\eta}\right)_{\eta=1}$$

With this, equation (21) becomes

$$\frac{t_w - t_b}{t_w - t_e} = -\sum_{n=0}^{\infty} \frac{b_n}{\beta_n}\left(\frac{dY_n}{d\eta}\right)_{\eta=1} \exp(-\beta_n\zeta) \tag{22}$$

By substituting equation (22) in equation (18), the expression for the Nusselt modulus becomes

$$Nu = \frac{4\sum_{n=0}^{\infty} b_n\left(\frac{dY_n}{d\eta}\right)_{\eta=1} \exp(-\beta_n\zeta)}{\sum_{n=0}^{\infty} \frac{b_n}{\beta_n}\left(\frac{dY_n}{d\eta}\right)_{\eta=1} \exp(-\beta_n\zeta)} \tag{23}$$

This completes the formulation of the equations yielding the important engineering quantities. Before numerical values of these quantities can be obtained, it is necessary to obtain the solution to equation (11a). It is clear from equations (11a) and (11b) that a different set of eigenvalues and eigenfunctions will be obtained for each pair of the rarefaction parameters $\xi_u/2L$ and $\xi_t/2L$.

Transverse Distribution Function $Y(\eta)$

Attention is now directed to the Sturm-Liouville eigenvalue problem (eq. (11a)). The function $Y(\eta)$ is the solution of this equation, subject to the boundary conditions (eq. (11b)) and the customary normalization convention $Y(0) \equiv 1$.

For convective heat transfer in laminar continuum channel flow, Dzung (ref. 6) and Sellars, et al. (ref. 7) have obtained asymptotic expressions for the eigenvalues and eigenfunctions through the use of the WKB method. A brief discussion of the WKB approximation and its application to the solution of eigenvalue equations in quantum theory may be found in reference 8. Asymptotic formulas for the eigenvalues and eigenfunctions for laminar heat transfer to slip flow in a parallel-plate channel with uniform wall heat flux have been derived in reference 3 by applying this method. The results were found to be in good agreement with numerical solutions obtained in the course of the investigation. Hence, it is of interest to apply this method to the present problem.

In accordance with the method of references 6 and 7, a solution of the following form is considered

$$Y(\eta) = \exp\left[m(\eta)\right] \tag{24a}$$

where

$$m = \sqrt{\beta}\, m_0 + m_1 + \frac{m_2}{\sqrt{\beta}} + \cdot \cdot \cdot \tag{24b}$$

and, since β is assumed to be large, only the first two terms of the previous series are retained. Then it can be shown that the asymptotic solution of equation (11a) is given by

$$Y(\eta) = \frac{A \exp\left[i \sqrt{\beta} \int_0^{\eta} f(\eta)^{\frac{1}{2}}\, d\eta\right] + B \exp\left[-i \sqrt{\beta} \int_0^{\eta} f(\eta)^{\frac{1}{2}}\, d\eta\right]}{f(\eta)^{\frac{1}{4}}} \qquad \text{for} \quad \sigma = 2,1 \tag{25}$$

where the coefficients A and B remain to be determined. It is noteworthy that, for continuum flow ($\lambda = 0$), a singularity exists in equation (25) at $\eta = 1$ for $\sigma = 2$ and $\sigma = 1$, since $\left[f(1)\right]_{\lambda=0} = 0$, and also at $\eta = 0$ for $\sigma = 1$, since $\left[f(0)\right]_{\substack{\lambda=0\\ \sigma=1}} = 0$. This behavior has required the development of alternative solutions, valid near $\eta = 0$ and $\eta = 1$ (refs. 6 and 7). For slip flow ($\lambda \neq 0$), the functions $f(\eta)$ are nowhere zero, and hence equation (25) has no singularities for slip flow. The accuracy of the approximation, however, (at least for the first few eigenconstants), might be expected to diminish as the slip velocity u_s approaches zero, since the effect of the singularity for $u_s = 0$ will undoubtedly come into play. Conversely, as the slip velocity increases from zero, equation (25) should become an increasingly more reasonable approximation of the actual equation, especially as β_n becomes large. Since it is anticipated that the coefficients A and B are different for the cases $\sigma = 2$ and $\sigma = 1$, each case will be considered separately.

For the case $\sigma = 2$, the coefficients A and B are determined from the continuation of equation (11a) to the channel central zone $\eta \approx 0$, where $Y(\eta)$ can be approximated by the cosine function and the conditions $Y(0) = 1$ and $(dY/d\eta)_{\eta=0} = 0$ are satisfied:

$$Y(\eta) \approx \cos \sqrt{\beta f(0)}\, \eta \qquad \text{for} \quad \eta^2 \ll 1 \tag{26}$$

where $f(0) = u_c/\bar{u} = (3/2)[(1 + 4\lambda)/(1 + 6\lambda)]$. Thus it is found that, to make equations (25) and (26) equal for small η, it is required that $A = B = [f(0)]^{1/4}/2$. Using this result and the first part of equation (3) gives

$$Y(\eta) = (1 + 4\lambda)^{1/4}(1 + 4\lambda - \eta^2)^{-1/4} \cos(\sqrt{\beta}\, I) \tag{27}$$

and

$$\frac{dY}{d\eta} \equiv Y'(\eta) = \frac{1}{2}(1 + 4\lambda)^{1/4}(1 + 4\lambda - \eta^2)^{-5/4}$$

$$\times \left[\eta \cos(\sqrt{\beta}\, I) - \frac{2\left(\frac{3}{2}\right)^{1/2}(1 + 4\lambda - \eta^2)^{3/2} \sqrt{\beta}\, I \sin(\sqrt{\beta}\, I)}{I(1 + 6\lambda)^{1/2}}\right] \tag{28}$$

where

$$I \equiv \int_0^\eta f(\eta)^{1/2}\, d\eta = \left(\frac{3}{8}\right)^{1/2} \frac{\eta(1 + 4\lambda - \eta^2)^{1/2} + (1 + 4\lambda)\sin^{-1}\left[\frac{\eta}{(1 + 4\lambda)^{1/2}}\right]}{(1 + 6\lambda)^{1/2}} \tag{29}$$

The values of the function Y and its slope $dY/d\eta$ at the upper wall are found by setting $\eta = 1$ in equations (27) and (28), respectively; the results are

$$Y(1) = \left(\frac{1 + 4\lambda}{4\lambda}\right)^{1/4} \cos \delta \tag{30}$$

$$\left(\frac{dY}{d\eta}\right)_{\eta=1} = \frac{1}{2} (1 + 4\lambda)^{1/4}(4\lambda)^{-5/4}\left[\cos \delta - \frac{2\left(\frac{3}{2}\right)^{1/2}(4\lambda)^{3/2} \delta \sin \delta}{I_1(1 + 6\lambda)^{1/2}}\right] \tag{31}$$

where

$$\delta \equiv \sqrt{\beta}\, I_1 \tag{32}$$

and

$$I_1 \equiv \int_0^1 f(\eta)^{1/2}\, d\eta = \left(\frac{3}{8}\right)^{1/2} \frac{(4\lambda)^{1/2} + (1 + 4\lambda)\sin^{-1}\left[\frac{1}{(1 + 4\lambda)^{1/2}}\right]}{(1 + 6\lambda)^{1/2}} \tag{33}$$

The eigenvalues are determined by the requirement $Y(1) = -2(\xi_t/2L)(dY/d\eta)_{\eta=1}$. Then, with equations (30) and (31) combined in accordance with this relation, the eigenvalues are obtained as roots of the characteristic equation

$$\delta_n \tan \delta_n = (4\lambda + \Gamma) \frac{\sqrt{4\lambda} + (1 + 4\lambda)\sin^{-1}\left(\frac{1}{\sqrt{1 + 4\lambda}}\right)}{4\Gamma(4\lambda)^{3/2}} \equiv E \tag{34}$$

where E, for given values of λ and Γ, is a constant. The first five roots of equation (34) are given in reference 9 for a number of values of E. The values of I_1 for any given slip velocity $u_s/\bar{u}$ are shown in figure 2. The eigenfunctions corresponding to these eigenvalues will be denoted by Y_n. It can be seen that the eigenvalues (and hence the eigenfunctions) depend on the two rarefaction parameters $\xi_u/2L$ and $\xi_t/2L$, as previously noted. This result differs from that obtained for the uniform-wall-heat-flux problem (ref. 3), where the eigenvalues and eigenfunctions were dependent only on the parameter $\xi_u/2L$.

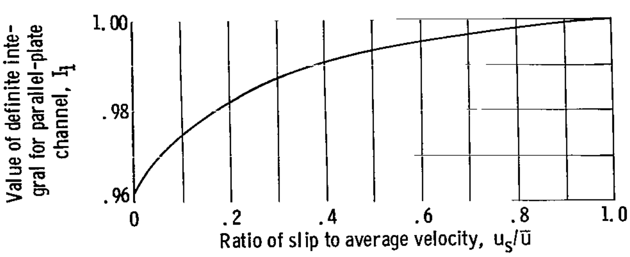

Figure 2. - Value of definite integral for parallel-plate channel for any value of ratio of slip to average velocity.

To obtain the series coefficients b_n (eq. (14)), it is necessary to evaluate the terms $(\partial Y/\partial\beta)_{\substack{\eta=1\\ \beta=\beta_n}}$ and $(\partial^2 Y/\partial\eta\ \partial\beta)_{\substack{\eta=1\\ \beta=\beta_n}}$. These expressions are determined by differentiating equations (30) and (31), respectively, with respect to β. The results may be written as

$$\left(\frac{\partial Y}{\partial\beta}\right)_{\substack{\eta=1\\ \beta=\beta_n}} = -\frac{(1 + 4\lambda)^{1/4}\ E \cos\ \delta_n}{(4\lambda)^{1/4}\ 2\beta_n} \tag{35a}$$

$$\left(\frac{\partial^2 Y}{\partial\beta\ \partial\eta}\right)_{\substack{\eta=1\\ \beta=\beta_n}} = -\frac{(1 + 4\lambda)^{1/4}\left[E + \dfrac{(4\lambda + \Gamma)(E + \delta_n^2)}{E\Gamma}\right]\cos\ \beta_n}{4\beta_n(4\lambda)^{5/4}} \tag{35b}$$

Thus, the coefficients b_n as evaluated from equation (14) are given as

$$b_n = \frac{8\lambda(4\lambda)^{1/4}}{(4\lambda + \Gamma)(1 + 4\lambda)^{1/4}\left(E + 1 + \dfrac{\delta_n^2}{E}\right)\cos\ \delta_n} \tag{36}$$

The slope $dY/d\eta$ evaluated at the wall, given by equation (31), can be alternatively expressed as

$$\left(\frac{dY_n}{d\eta}\right)_{\eta=1} = -\frac{(1 + 4\lambda)^{1/4}\ \cos\ \delta_n}{(4\lambda)^{1/4}\ 2\Gamma} \tag{37}$$

It is convenient to define a new coefficient B_n, given by the product of b_n and $(dY/d\eta)_{\eta=1}$, as

$$B_n \equiv b_n\left(\frac{dY_n}{d\eta}\right)_{\eta=1} = \frac{-4\lambda}{\Gamma(4\lambda + \Gamma)\left(E + 1 + \dfrac{\delta_n^2}{E}\right)} \tag{38}$$

Equations (30), (34), and (38) can be used to calculate the constants $Y_n(1)$, eigenvalues β_n, and coefficients B_n for given values of $\xi_u/2L$ and $\xi_t/2L$. In the interests of a unified presentation of results, however, such calculations will be delayed until after the unsymmetrical case $\sigma = 1$ has been treated.

For the unsymmetrical case, the formal asymptotic solution (eq. (25)) is first continued to the insulated wall $\eta = 0$, where again $Y(\eta)$ can be approximated by the cosine function

$$Y(\eta) \approx \cos\left[\sqrt{\beta f(0)}\ \eta\right] \qquad \text{for} \quad \eta^2 \ll 1 \tag{26}$$

The coefficients A and B are readily determined to be $A = B = [f(0)]^{1/4}/2$ so that

$$Y(\eta) = \lambda^{1/4}(\eta - \eta^2 + \lambda)^{-1/4} \cos(\sqrt{\beta}\ J) \tag{39}$$

and

$$\frac{dY}{d\eta} = -\lambda^{1/4}(\eta - \eta^2 + 4\lambda)^{-5/4}\ \frac{(1 - 2\eta)\cos(\sqrt{\beta}\ J) + \dfrac{4(\eta - \eta^2 + \lambda)^{3/2}\ \sqrt{6}\ \sqrt{\beta}\ J \sin(\sqrt{\beta}\ J)}{J\ \sqrt{1 + 6\lambda}}}{4} \tag{40}$$

where

$$J \equiv \int_0^\eta f(\eta)^{1/2}\ d\eta = \sqrt{\frac{3}{8}}\left[\sqrt{\lambda} + (2\eta - 1)\sqrt{\eta - \eta^2 + \lambda} - (1 + 4\lambda)\ \frac{\sin^{-1}\left(\dfrac{1 - 2\eta}{\sqrt{1 + 4\lambda}}\right) - \sin^{-1}\left(\dfrac{1}{\sqrt{1 + 4\lambda}}\right)}{2}\right] \tag{41}$$

The function Y and its derivative $dY/d\eta$ are evaluated at the upper wall by setting $\eta = 1$ in equations (39) and (40), which results in

$$Y(1) = \cos\epsilon \tag{42}$$

$$\left(\frac{dY}{d\eta}\right)_{\eta=1} = -\ \frac{-\cos\epsilon + \dfrac{4\lambda^{3/2}\ \sqrt{6}\ \epsilon \sin\epsilon}{J_1\ \sqrt{1 + 6\lambda}}}{4\lambda} \tag{43}$$

where

$$\epsilon \equiv \sqrt{\beta}\ J_1 \tag{44}$$

and

$$J_1 \equiv \int_0^1 f(\eta)^{1/2}\, d\eta = \left(\frac{3}{8}\right)^{1/2} \frac{(4\lambda)^{1/2} + (1 + 4\lambda)\sin^{-1} \frac{1}{(1 + 4\lambda)^{1/2}}}{(1 + 6\lambda)^{1/2}}$$

$$= I_1 \tag{45}$$

The eigenvalues for the present case ($\sigma = 1$) are determined by the requirement that $Y(1) = -(\xi_t/2L)(dY/d\eta)_{\eta=1}$. Then, by combining equations (42) and (43) in accordance with this requirement, the eigenvalues β_n are obtained as roots of the characteristic equation

$$\epsilon_n \tan \epsilon_n = (4\lambda + \Gamma) \frac{\sqrt{4\lambda} + (1 + 4\lambda)\sin^{-1}\left(\frac{1}{\sqrt{1 + 4\lambda}}\right)}{2\Gamma(4\lambda)^{3/2}}$$

$$\equiv F$$

$$= 2E \tag{46}$$

where $\epsilon_n = \sqrt{\beta_n}\, J_1$.

The expressions $(\partial Y/\partial\beta)_{\substack{\eta=1 \\ \beta=\beta_n}}$ and $(\partial^2 Y/\partial\beta\, \partial\eta)_{\substack{\eta=1 \\ \beta=\beta_n}}$, necessary for the evaluation of the coefficients b_n, can be obtained readily from the equations developed so far as

$$\left(\frac{\partial Y}{\partial \beta}\right)_{\substack{\eta=1 \\ \beta=\beta_n}} = -\frac{F \cos \epsilon_n}{2\beta_n} \tag{47a}$$

$$\left(\frac{\partial^2 Y}{\partial \beta\, \partial \eta}\right)_{\substack{\eta=1 \\ \beta=\beta_n}} = -\cos \epsilon_n \frac{F + \frac{(4\lambda + \Gamma)(F + \epsilon_n^2)}{F\Gamma}}{8\lambda\beta_n} \tag{47b}$$

The series coefficients b_n are thus given by

$$b_n = \frac{8\lambda}{(4\lambda + \Gamma)\left(F + 1 + \frac{\epsilon_n^2}{F}\right)\cos \epsilon_n} \tag{48}$$

Equation (43) can be recast into the form

TABLE I. - EIGENVALUES AND CONSTANTS FOR SLIP FLOW IN CHANNEL WITH UNIFORM WALL TEMPERATURES

	Ratio of slip to average velocity, $u_s/\overline{u}$							
	1/3				3/5			
	Temperature-jump coefficient, $\xi_t/2L$							
	0.1333		0.5333		0.4		1.6	
	Solution							
	Analytical	Numerical	Analytical	Numerical	Analytical	Numerical	Analytical	Numerical
	Symmetry number, 2							
$\sqrt{\beta_1}$	1.431	1.168	1.289	0.8128	1.111	0.9087	0.8750	0.5273
$\sqrt{\beta_2}$	4.321	4.083	4.010	3.630	3.705	3.602	3.451	3.337
$\sqrt{\beta_3}$	7.265	7.085	6.906	6.682	6.645	6.586	6.475	6.417
$\sqrt{\beta_4}$	10.28	10.14	9.945	9.794	9.700	9.661	9.581	9.541
$Y_1(1)$	.2163	.2926	.4045	.6358	.5320	.5767	.7640	.8506
$Y_2(1)$	-.6028	-.6917	-.9410	-1.082	-1.019	-1.016	-1.135	-1.124
$Y_3(1)$	.8508	.9340	1.185	1.227	1.123	1.120	1.173	1.164
$Y_4(1)$	-1.0195	-1.0823	-1.264	-1.293	-1.151	-1.153	-1.180	-1.176
$Y_1'(1)$	-.8120	-1.098	-.3795	-.5961	-.6645	-.7208	-.2388	-.2658
$Y_2'(1)$	2.265	2.594	.8835	1.014	1.270	1.270	.3550	.3534
$Y_3'(1)$	-3.295	-3.503	-1.110	-1.150	-1.408	-1.400	-.3665	-.3635
$Y_4'(1)$	3.820	4.060	1.185	1.213	1.440	1.442	.3692	.3674
b_1	.6475	1.177	.4930	1.096	.7085	1.124	.3639	1.044
b_2	-.1968	-.2526	-.1324	-.1257	-.1510	-.1635	-.0507	-.0554
b_3	.1059	.1164	.0575	.0438	.0560	.0570	.0157	.0154
b_4	-.0654	-.0669	-.0312	-.0218	-.0227	-.0278	-.0073	-.0073
	Symmetry number, 1							
$\sqrt{\beta_1}$	1.498	1.376	1.420	1.048	1.295	1.136	1.092	0.7149
$\sqrt{\beta_2}$	4.520	4.394	4.295	3.933	4.005	3.904	3.675	3.529
$\sqrt{\beta_3}$	7.545	7.435	7.225	6.966	6.900	6.844	6.625	6.565
$\sqrt{\beta_4}$	10.58	10.50	10.23	10.05	9.905	9.872	9.680	9.648
$Y_1(1)$	.0872	.1900	.1651	.4984	.2790	.4206	.4648	.7550
$Y_2(1)$	-.2419	-.3907	-.4540	-.7767	-.6626	-.7503	-.8669	-.9491
$Y_3(1)$	.3827	.5267	.6561	.8696	.8387	.8740	.9563	.9788
$Y_4(1)$	-.5000	-.6262	-.7660	-.9137	-.9272	-.9063	-.9782	-.9886
$Y_1'(1)$	-.6545	-1.425	-.3200	-.9345	-.6975	-1.052	-.2900	-.4722
$Y_2'(1)$	1.811	2.931	.8500	1.456	1.658	1.876	.5400	.5932
$Y_3'(1)$	-2.869	-3.951	-1.230	-1.631	-2.099	-2.185	-.5975	-.6118
$Y_4'(1)$	3.750	4.697	1.438	1.713	2.268	2.318	.6115	.6183
b_1	.8575	1.228	.6299	1.147	.8720	1.180	.3950	1.0766
b_2	-.2942	-.3412	-.1910	-.2032	-.2399	-.2508	-.0815	-.0992
b_3	.1691	.1829	.0986	.0852	.1065	.1063	.0294	.0330
b_4	-.1140	-.1176	-.0605	-.0469	-.0582	-.0570	-.0144	-.0161

$$\left(\frac{dY}{d\eta}\right)_{\substack{\eta=1\\ \beta=\beta_n}} = -\frac{\cos \epsilon_n}{\Gamma} \tag{49}$$

so that

$$B_n \equiv b_n\left(\frac{dY}{d\eta}\right)_{\substack{\eta=1\\ \beta=\beta_n}} = -\frac{8\lambda}{\Gamma(4\lambda + \Gamma)\left(F + 1 + \frac{\epsilon_n^2}{F}\right)} \tag{50}$$

Equations (30), (34), and (38), for $\sigma = 2$, or equations (42), (46), and (50), for $\sigma = 1$, in conjunction with figure 2 (p. 11) contain all the information essential to the determination of the variation in the gas temperature adjacent to the wall (eq. (10)), the wall heat-flux variation (eq. (16)), and the Nusselt modulus (eq. (23)) along the length of the channels. These expressions for the eigenvalues, eigenfunctions, and coefficients are remarkably simple in form and lead to relative ease of computation. The level of accuracy of the expressions remains to be determined.

The first four eigenvalues and important constants are given in table I for several different values of the parameters $u_s/\bar{u}$ and $\xi_t/2L$ for the cases of a step change in temperature at both plates, $\sigma = 2$, and at the upper plate only (while the lower wall is insulated), $\sigma = 1$. The particular numerical values chosen for $u_s/\bar{u}$ and $\xi_t/2L$ correspond to values for the rarefaction parameter $\mu\sqrt{R_g t}/2pL$ of 0.0667 and 0.2, $\gamma = 1.4$, Pr = 0.73, g = 1, and a = 1 and 0.4. Although the value of 0.2 for the rarefaction parameter may be outside the slip-flow regime, it has been included since at lower densities, in the beginning of the transition regime, prior findings suggest that slip-flow solutions may remain fairly good. Results for $u_s/\bar{u} = 1$ (slug flow) would definitely be outside the slip-flow regime, since for $u_s/\bar{u} = 1$, $l/2L \to \infty$. The results for continuum flow ($\xi_u/2L = \xi_t/2L = 0$) are given in table II and were obtained from reference 6.

TABLE II. - EIGENVALUES AND COEFFICIENTS FOR CONTINUUM FLOW IN PARALLEL-PLATE CHANNEL WITH UNIFORM WALL TEMPERATURE

[Data from ref. 6.]

	Symmetry number	
	2	1
$\sqrt{\beta_1}$	1.372	1.557
$\sqrt{\beta_2}$	4.625	4.855
$\sqrt{\beta_3}$	7.89	8.14
$\sqrt{\beta_4}$	11.16	11.40
$-B_1$	1.708	2.167
$-B_2$	1.138	1.434
$-B_3$	.951	1.193
$-B_4$	.848	1.064

To check the level of accuracy of the slip-flow results, equation (11a) was solved numerically, by the Runge-Kutta method, on an IBM 7094 digital computer. The forward integration was started by using the boundary condition (eq. (11b)) at $\eta = 0$ and the normalization convention $Y_n(0) \equiv 1$. The eigenvalues were found by trial and error until the second boundary condition of equation (11b) was satisfied at $\eta = 1$. The first four eigenvalues and constants are given in table I for the same choice of slip-flow parameters.

The analytical expressions presented herein were derived on the assumption that β_n is large and, hence, are valid only in that limit. There is, however, substantial agreement between the relevant quantities computed from the analytical expressions and the numerical solutions even for values of n as low as 3. Although the agreement is good for $\sqrt{\beta_2}$ when $u_s/\bar{u} = 3/5$ and fair for $Y_2(1)$, $Y_2'(1)$, and b, it is only fair for $\sqrt{\beta_2}$ when $u_s/\bar{u} = 1/3$ and somewhat poor for the other quantities. Thus, the extent of agreement depends on the parameters $u_s/\bar{u}$ and $\xi_t/2L$, the best agreement being at low values of $\xi_t/2L$ and higher values of $u_s/\bar{u}$. It is evident from these comparisons, however, that the analytical expressions presented here have definite application to determining the higher eigenvalues for laminar heat transfer in channels under slip-flow conditions.

With the numerical information in tables I and II, the variation of the temperature of the gas adjacent to the upper wall along the length of the channels has been evaluated from equation (10) by setting $\eta = 1$, and plots are given in figure 3 for $\sigma = 2$ and 1.

In the absence of rarefaction effects, the difference between the surface temperature t_w and the contiguous gas temperature t_g is zero along the entire length of the channels. With rarefaction, the temperature difference $t_g - t_w$ has nonzero values, decreasing from $t_e - t_w$ with increasing distance from the heated section entrance. The effect of an increase in rarefaction is to increase $t_g - t_w$ toward the maximum difference $t_e - t_w$ at any given axial location. The direction of this effect is physically reasonable, since

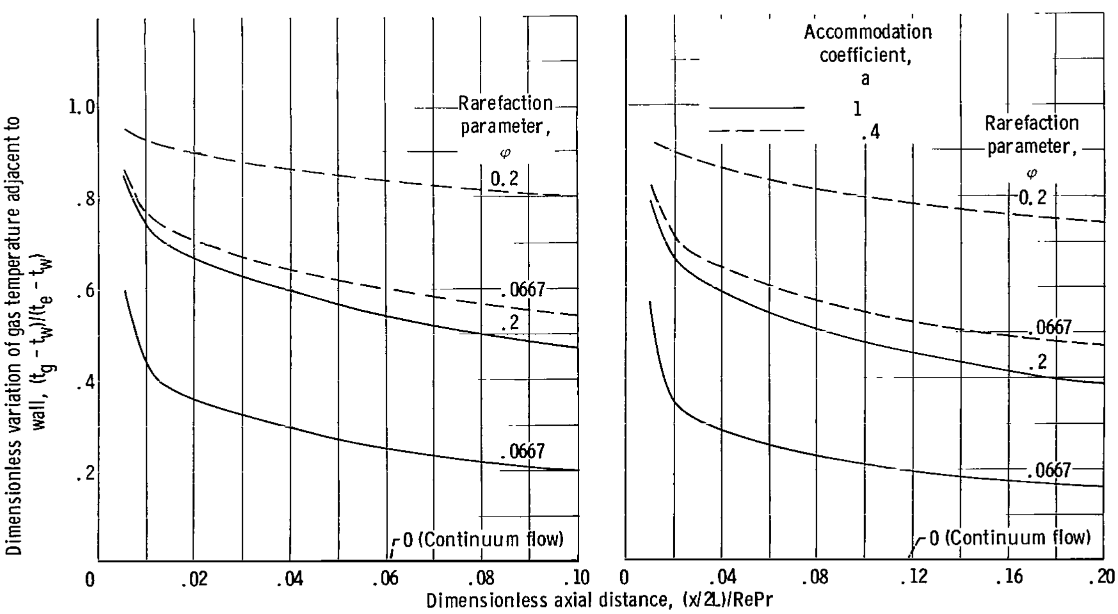

(a) Symmetry number, 2.

(b) Symmetry number, 1.

Figure 3. - Variation of gas temperature adjacent to wall for flow in parallel-plate channel. Specular reflection coefficient, 1; ratio of specific heats, 1.4; Prandtl number, 0.73.

the temperature jump can be considered as an effective thermal contact resistance at the gas-surface interface. The value of the accommodation coefficient also has an important effect on the variation of $t_g - t_w$ with axial distance, and this is associated with the increase in temperature-jump effect with a decrease in accommodation coefficient. For both wall-temperature-change situations, the temperature difference $t_g - t_w$ varies significantly over approximately the first 10 percent of the dimensionless distance considered and then varies more slowly over the remaining distance. This result suggests that the thermal creep velocity, which has been neglected in the present investigation, would have its greatest effect concentrated in the region $(x/2L)/\mathrm{RePr} \leq 0.01$ for $\sigma = 2$, or $(x/2L)/\mathrm{RePr} \leq 0.02$ for $\sigma = 1$.

The wall heat-flux variation required to maintain the wall temperature constant has been evaluated from equation (16) by using the data of tables I and II and has been plotted in figure 4 for $\sigma = 2$ and 1. An increase in gas rarefaction and/or a decrease in the value of the accommodation coefficient produces a decrease in the heat-flux requirement, at a given axial position, over that for continuum gas flow. This is reasonable, since the thermal contact resistance effect of the temperature jump tends to overpower the decrease in thermal resistance associated with velocity slip (especially if the accommodation coefficient has a lower specified value) and thus increases the resistance to heat transfer to the gas from the wall; consequently, the wall heat-flux requirement decreases. The wall heat-flux requirement, at a given axial position, however, is slightly greater for the channel with a wall temperature change at the upper wall only than for the channel with a step change in temperature at both walls.

The variation in local Nusselt number along the channels can be evaluated from equation (23) and from the numerical information in tables I and II. The fully developed heat-transfer condition occurs for $x/2L$ sufficiently large so

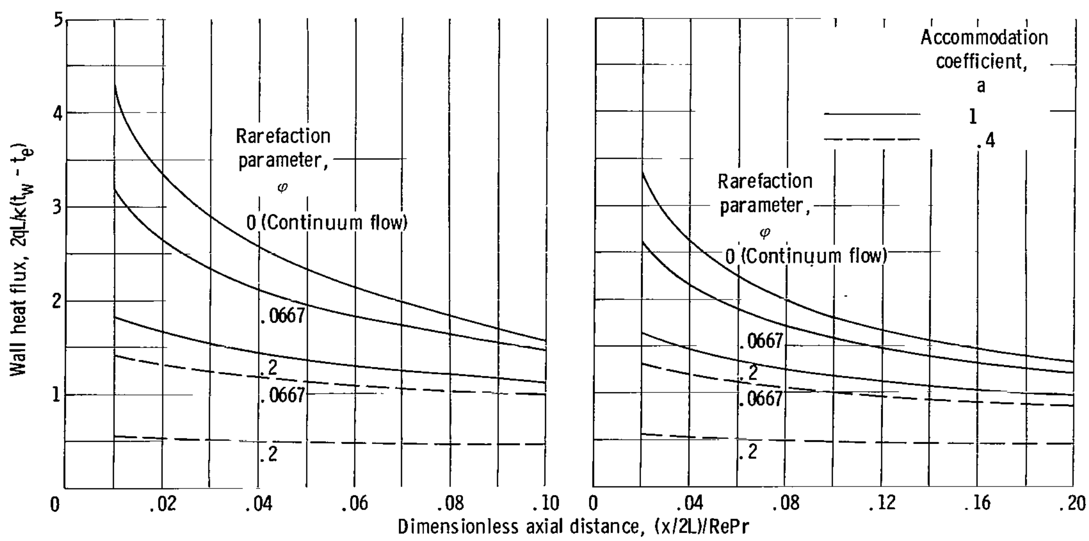

(a) Symmetry number, 2.

(b) Symmetry number, 1.

Figure 4. - Variation of wall heat flux following step change in wall temperature for slip flow in parallel-plate channel. Specular reflection coefficient, 1; ratio of specific heats, 1.4; Prandtl number, 0.73.

that only the first term of the series need be considered. Then the fully developed Nusselt number follows as the simple expression $Nu_d = 4\beta_1$. Fully developed Nusselt numbers thus obtained have been plotted in figure 5 as a function of $\mu\sqrt{R_g t}/2pL$ in the form of a ratio $(Nu/Nu_0)_d$, where Nu_0 represents the continuum value 7.53 for $\sigma = 2$ or 9.70 for $\sigma = 1$. The effect of gas rarefaction is to decrease the value of the Nusselt number below its continuum value, and the reduction increases significantly with increasing mean free path. It is noteworthy that the effects of gas rarefaction are more pronounced in the channel with both walls step-changed in temperature than in the channel with a change in temperature at the upper wall only. The effect on the Nusselt number of the specified value of the accommodation coefficient is evident.

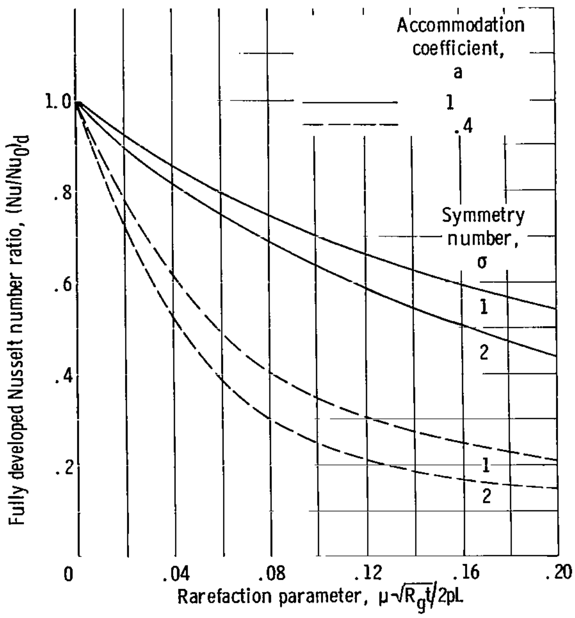

Figure 5. - Fully developed Nusselt number ratio for flow in channel at uniform wall temperature. Specular reflection coefficient, 1; ratio of specific heats, 1.4; Prandtl number, 0.73.

The variation in Nusselt number along the channel with a step change in wall temperature at one or both walls has been evaluated and plotted in figure 6. The effect of the gas rarefaction is always to decrease the Nusselt number below its continuum value at every position along the heated length. It is interesting to note that the Nusselt number variation for both $\sigma = 2$ and $\sigma = 1$ exhibits trends similar to those observed for channels with uniform wall heat flux at one or both walls (ref. 3). The values of Nu for uniform wall temperature, however, lie somewhat lower than those for uniform wall heat flux for both $\sigma = 2$ and $\sigma = 1$, with differences becoming negligible for higher values of $\mu\sqrt{R_g t}/2pL$ and lower values of a.

RAREFIED GAS FLOW IN A CIRCULAR TUBE WITH STEP CHANGE IN WALL TEMPERATURE

Attention is now directed to the fully developed laminar flow of a slightly rarefied gas through a circular tube as illustrated in figure 7. For $x < 0$ the tube and the gas are assumed to be isothermal at temperature t_e, whereas for $x \geq 0$ the tube is step-changed to a new value of t_w.

The energy equation analogous to equation (1) is

$$u\frac{\partial t}{\partial x} = \frac{\alpha}{r}\frac{\partial}{\partial r}\frac{r\,\partial t}{\partial r} \tag{51}$$

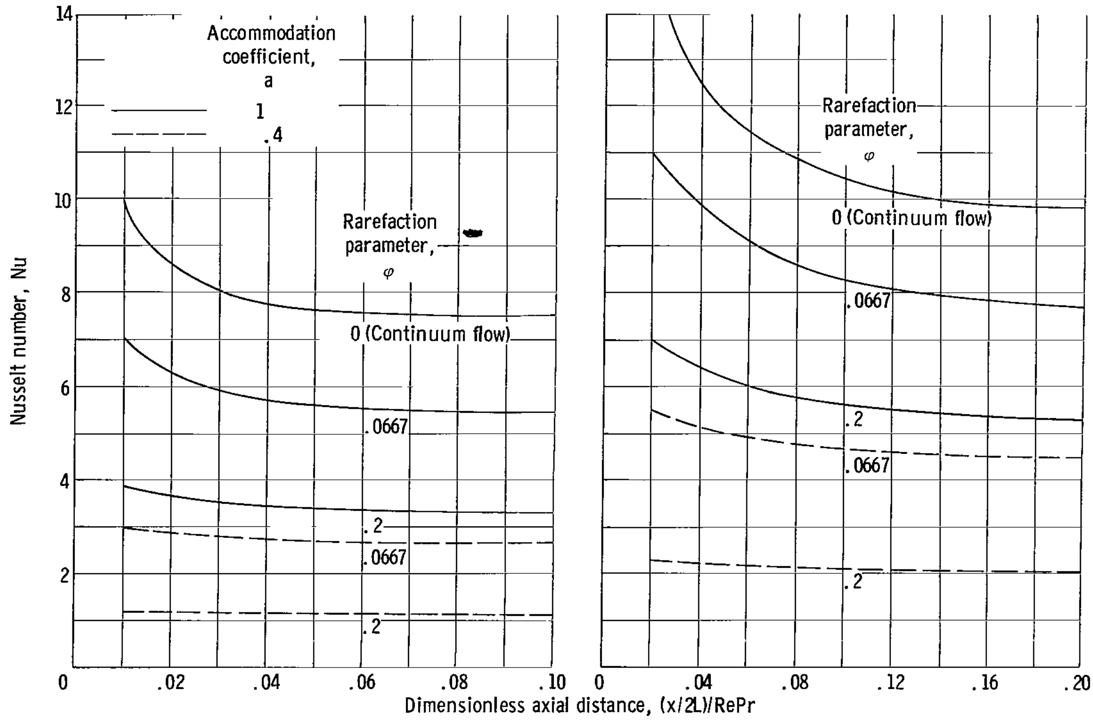

(a) Symmetry number, 2. (b) Symmetry number, 1.

Figure 6. - Variation of local Nusselt number along channel for uniform wall temperature. Specular reflection coefficient, 1; ratio of specific heats, 1.4; Prandtl number, 0.73.

This is rewritten in terms of dimensionless variables to yield

$$2f(\omega)\frac{\partial T}{\partial \psi} = \frac{1}{\omega}\frac{\partial}{\partial \omega}\left(\omega\frac{\partial T}{\partial \omega}\right) \tag{52}$$

The velocity distribution, slip velocity, and average velocity have been given in reference 1. The use of these expressions leads to the dimensionless velocities $u/\overline{u}$ and $u_s/\overline{u}$ as

$$\left.\begin{aligned} \frac{u}{\overline{u}} &\equiv f(\omega) = 2\,\frac{1-\omega^2+4\theta}{1+8\theta} \\ \frac{u_s}{\overline{u}} &= f(1) = \frac{8\theta}{1+8\theta} \end{aligned}\right\} \text{for} \quad \theta \equiv \xi_u/d \tag{53}$$

Equation (52) is to be solved subject to boundary conditions similar to those specified for the parallel-plate channel

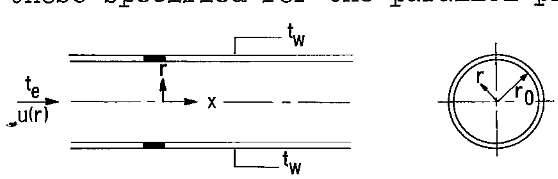

Figure 7. - Physical model and coordinate system for circular tube.

$$\left.\begin{aligned} T &= 1 \qquad \text{at} \quad \psi = 0 \quad \text{for all} \quad \omega \\ \frac{\partial T}{\partial \omega} &= 0 \qquad \text{at} \quad \omega = 0 \quad \text{for} \quad \psi \geq 0 \end{aligned}\right\} \tag{54a}$$

and

$$T(1) = -2 \frac{\xi_t}{d} \left(\frac{\partial T}{\partial \omega} \right)_{\omega=1} \qquad \text{at} \quad \omega = 1 \tag{54b}$$

Equation (54b) arises from consideration of the temperature-jump condition at the tube wall.

A product solution of equation (52) of the following form is employed

$$T = X(\psi) \cdot R(\omega) \tag{55}$$

When this is inserted into equation (52), the solution for T can be written as

$$T = \frac{t - t_w}{t_e - t_w} = \sum_{m=1}^{\infty} c_m R_m(\omega) \exp(-\beta_m \psi) \tag{56}$$

where the β_m and R_m are the eigenvalues and corresponding eigenfunctions of the Sturm-Liouville system

$$\frac{d}{d\omega} \left(\omega \frac{dR_m}{d\omega} \right) + 2\beta_m \omega f(\omega) R_m = 0 \tag{57a}$$

with the boundary conditions

$$\left. \begin{aligned} \frac{dR_m}{d\omega} &= 0 \qquad \text{at} \quad \omega = 0 \\ R_m(1) &= -2 \frac{\xi_t}{d} \left(\frac{dR_m}{d\omega} \right)_{\omega=1} \end{aligned} \right\} \tag{57b}$$

The coefficients c_m are evaluated from the boundary condition that $T = 1$ at the tube entrance ($\psi = 0$). Applying this condition to equation (56), it is found that c_m must satisfy

$$1 = \sum_{m=1}^{\infty} c_m R_m(\omega) \tag{58}$$

From the properties of the Sturm-Liouville system, it follows immediately that

$$c_m = \frac{\int_0^1 2\omega f(\omega) R_m \, d\omega}{\int_0^1 2\omega f(\omega) R_m^2 \, d\omega} \tag{59}$$

The technique used for evaluating the coefficients b_n for the parallel-plate channel (appendix B) is completely applicable here, and it can be shown that the solution for the coefficients c_m reduces to

$$c_m = \frac{-1}{\beta_m\left(\frac{\partial R}{\partial \beta} + 2\,\frac{\xi_t}{d}\,\frac{\partial^2 R}{\partial \beta\,\partial \omega}\right)_{\substack{\omega=1\\ \beta=\beta_m}}} \tag{60}$$

The functions $R_m(\omega)$ and the corresponding eigenvalues β_m are as yet undetermined. The analysis will be extended at this point, however, to the formulation of the quantities of engineering interest. From the temperature distribution given by equation (56), the axial variation of the gas temperature adjacent to the wall, the wall heat-flux variation required to maintain the wall temperature constant, and the Nusselt number variation along the tube length may be computed from their respective definitions:

$$\frac{t_g - t_w}{t_e - t_w} = \sum_{m=1}^{\infty} c_m R_m(1)\exp(-\beta_m \psi) \tag{61}$$

$$q = \kappa\left(\frac{\partial t}{\partial r}\right)_{r=r_0}$$

$$= -\frac{\kappa(t_w - t_e)}{r_0}\sum_{m=1}^{\infty} c_m\left(\frac{dR_m}{d\omega}\right)_{\omega=1}\exp(-\beta_m \psi) \tag{62}$$

$$\mathrm{Nu} \equiv \frac{hd}{\kappa}$$

$$= \frac{qd}{\kappa(t_w - t_b)}$$

$$= 2\,\frac{\displaystyle\sum_{m=1}^{\infty} c_m\left(\frac{dR_m}{d\omega}\right)_{\omega=1}\exp(-\beta_m \psi)}{\displaystyle\sum_{m=1}^{\infty}\left(\frac{c_m}{\beta_m}\right)\left(\frac{dR_m}{d\omega}\right)_{\omega=1}\exp(-\beta_m \psi)} \tag{63}$$

RADIAL DISTRIBUTION FUNCTION $R(\omega)$

To determine the behavior of equation (57) (at large parameter β), the method used in solving the parallel-plate system can be adopted practically unchanged. The results are

$$R(1) = \sqrt{2}\left(\frac{1 + 8\theta}{4\theta}\right)^{1/4} \frac{\cos\tau + \sin\tau}{2\sqrt{\pi}\,\beta^{1/4}} \tag{64}$$

and

$$\left(\frac{dR}{d\omega}\right)_{\omega=1} = \sqrt{2}\left(\frac{1 + 8\theta}{4\theta}\right)^{1/4} \frac{(1 - 4\theta)(\cos\tau + \sin\tau) - 4\tau(4\theta)^{3/2}\dfrac{\sin\tau - \cos\tau}{K_1\sqrt{1 + 8\theta}}}{16\theta\sqrt{\pi}\,\beta^{1/4}} \tag{65}$$

where

$$\tau \equiv \sqrt{\beta}\, K_1 \tag{66}$$

$$K_1 \equiv \int_0^1 \left[2f(\omega)\right]^{1/2} d\omega = \frac{\sqrt{4\theta} + (1 + 4\theta)\sin^{-1}\left(\dfrac{1}{\sqrt{1 + 4\theta}}\right)}{\sqrt{1 + 8\theta}} \tag{67}$$

The eigenvalues are determined from the second boundary condition given in equation (57b), which requires that

$$R(1) = -2\,\frac{\xi_t}{d}\left(\frac{dR}{d\omega}\right)_{\omega=1}$$

Hence, combining equations (64) and (65) in accordance with this requirement, the eigenvalues β_m are obtained as roots of the characteristic equation

$$\tan\tau_m = \frac{M\tau_m + N}{M\tau_m - N} \tag{68}$$

where

$$
\left.\begin{aligned}
\tau_m &= \sqrt{\beta_m}\, K_1 \\
M &\equiv \frac{4(4\theta)^{3/2} \frac{\xi_t}{d}}{\sqrt{4\theta} + (1 + 4\theta)\sin^{-1}\left(\frac{1}{\sqrt{1 + 4\theta}}\right)} \\
N &\equiv 4\theta + (1 - 4\theta)\frac{\xi_t}{d}
\end{aligned}\right\} \tag{69}
$$

The values of K_1 for any given slip velocity $u_s/\bar{u}$ are shown in figure 8. The eigenvalues and eigenfunctions for the circular-tube problem depend on the two rarefaction parameters ξ_u/d and ξ_t/d.

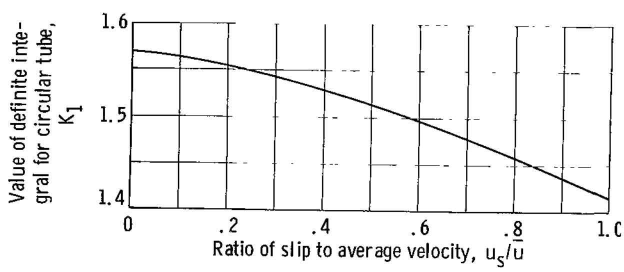

Figure 8. - Value of definite integral for circular tube for any value of ratio of slip to average velocity.

From the equations presented so far, the expressions $(\partial R/\partial\omega)_{\substack{\omega=1\\ \beta=\beta_m}}$ and $(\partial^2 R/\partial\omega\,\partial\beta)_{\substack{\omega=1\\ \beta=\beta_m}}$ can readily be evaluated; however, in the interests of a concise presentation, the evaluations will be omitted here. From the results, the coefficients c_m are evaluated from equation (60) as

$$
c_m = 4\sqrt{\pi}\,\beta_m^{1/4}\left(\frac{4\theta}{1 + 8\theta}\right)^{1/4} \frac{4\theta \dfrac{M\tau_m - N}{MN + N^2 + M^2\tau_m^2}}{\sqrt{2}\,\tau_m \cos\tau_m} \tag{70}
$$

The slope $dR/d\omega$ evaluated at the tube wall (eq. (65)) can be alternatively expressed as

$$
\left(\frac{dR}{d\omega}\right)_{\substack{\omega=1\\ \beta=\beta_m}} = -\sqrt{2}\left(\frac{1 + 8\theta}{4\theta}\right)^{1/4} \tau_m \cos\tau_m \frac{\dfrac{M}{\frac{\xi_t}{d}(M\tau_m - N)}}{\sqrt{\pi}\,\beta_m^{1/4}} \tag{71}
$$

Hence

$$
C_m \equiv c_m\left(\frac{dR}{d\omega}\right)_{\omega=1} = \frac{-16\theta}{\frac{\xi_t}{d}\left(N + \frac{N^2}{M} + M\tau_m^2\right)} \tag{72}
$$

Table III shows the first four eigenvalues and constants for slip flow in a circular tube. The results for continuum flow ($u_s/\overline{u} = 0$) are presented in table IV and were obtained from reference 10. Also shown in table III are the data obtained through the use of an IBM 7094 computer by the Runge-Kutta method. The numerical solutions were carried out in a manner which parallels that already described for the parallel-plate channel system. It should be noted that $R_m(0) = 1$ for all m. The asymptotic formula for β_m yields values of sufficient accuracy for $m \geq 2$, while the agreement for the various constants depends on the parameters $u_s/\overline{u}$ and ξ_t/d. The variation of the temperature of the gas adjacent to the wall along the length of the tube has been evaluated and plotted in figure 9. The trends are qualitatively similar to those evident in the parallel-plate channel system.

TABLE III. - EIGENVALUES AND CONSTANTS FOR SLIP FLOW IN TUBE WITH UNIFORM WALL TEMPERATURE

	Ratio of slip to average velocity, $u_s/\overline{u}$							
	2/5				2/3			
	Temperature-jump coefficient, ξ_t/d							
	0.1333		0.5333		0.4		1.6	
	Solution							
	Analytical	Numerical	Analytical	Numerical	Analytical	Numerical	Analytical	Numerical
$\sqrt{\beta_1}$	1.373	1.205	1.208	0.8287	1.065	0.9372	0.7600	0.5331
$\sqrt{\beta_2}$	3.260	3.085	2.980	2.750	2.885	2.837	2.695	2.663
$\sqrt{\beta_3}$	5.155	5.029	4.905	4.755	4.895	4.882	4.780	4.774
$\sqrt{\beta_4}$	7.100	7.008	6.875	6.782	6.975	6.964	6.875	6.887
$R_1(1)$	.1840	.2472	.3740	.5979	.5085	.5472	.8050	.8406
$R_2(1)$	-.2340	-.2773	-.3961	-.4287	-.4125	-.4070	-.4520	-.4406
$R_3(1)$	.2581	.2723	.3485	.3509	.3300	.3252	.3400	.3353
$R_4(1)$	-.2588	-.2582	-.3081	-.3040	-.2780	-.2765	-.2835	-.2809
$R_1'(1)$	-.6650	-.9273	-.3480	-.5608	-.6260	-.6838	-.2515	-.2627
$R_2'(1)$	1.006	1.040	.3725	.4019	.5140	.5086	.1445	.1377
$R_3'(1)$	-1.063	-1.021	-.3210	-.3290	-.4170	-.4062	-.1070	-.1048
$R_4'(1)$	1.030	.9682	.2908	.2849	.3460	.3453	.0926	.0878
c_1	.9150	1.408	.4845	1.201	.9595	1.250	.5445	1.079
c_2	-.4185	-.6471	-.2282	-.2896	-.3471	-.3585	-.1050	-.1077
c_3	.3300	.3978	-.1325	.1385	.1695	.1702	.0460	.0442
c_4	-.2419	-.2738	-.0825	-.0838	-.1045	-.1041	-.0259	-.0242

TABLE IV. - EIGENVALUES AND COEFFICIENTS FOR CONTINUUM FLOW IN CIRCULAR TUBE WITH UNIFORM WALL TEMPERATURE

[Data from ref. 10]

$\sqrt{\beta_1}$	1.351
$\sqrt{\beta_2}$	3.340
$\sqrt{\beta_3}$	5.337
$\sqrt{\beta_4}$	7.336
$-C_1$	1.500
$-C_2$	1.088
$-C_3$	.9255
$-C_4$	.8308

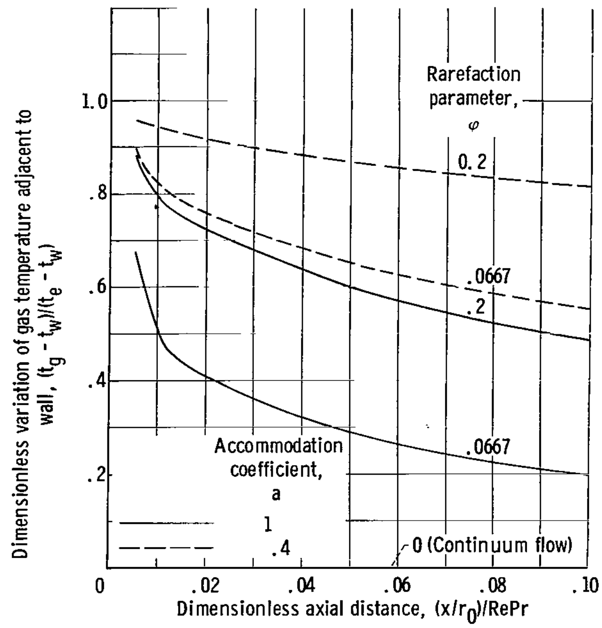

Figure 9. - Variation of gas temperature adjacent to wall for slip flow in circular tube. Specular reflection coefficient, 1; ratio of specific heats, 1.4; Prandtl number, 0.73.

The wall heat-flux variation required to maintain the tube wall temperature constant is shown in figure 10. Increased gas rarefaction and/or decreased value of accommodation coefficient decrease the heat-flux requirement, as was the case in the parallel-plate channel system.

The variation in Nusselt number along the tube with a step change in wall temperature has been evaluated and plotted in figure 11. Also shown are asymptotes for the fully developed values (achieved for $x \rightarrow \infty$). For the values of the parameter $\mu \sqrt{R_g t}/pd$ considered, the Nusselt number for $(x/r_0)/RePr \geq 0.10$ differs little from the fully developed value.

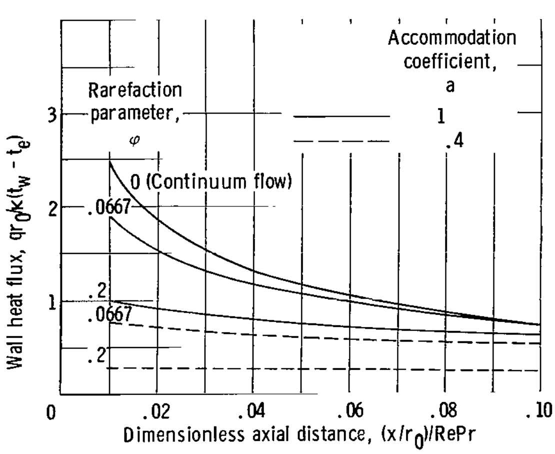

Figure 10. - Variation of wall heat flux following step change in wall temperature for slip flow in circular tube. Specular reflection coefficient, 1; ratio of specific heats, 1.4; Prandtl number, 0.73.

DISCUSSION OF UNIFORM WALL HEAT-FLUX AND UNIFORM WALL-TEMPERATURE RESULTS

It is illuminating to present a qualitative picture of the uniform wall heat-flux and uniform wall-temperature results under slip-flow conditions in order that the significant physical mechanisms and features of gas rarefaction stand out more clearly, unobscured by the mathematics. To this end, the results of reference 3 and the present results are presented and compared in a qualitative fashion.

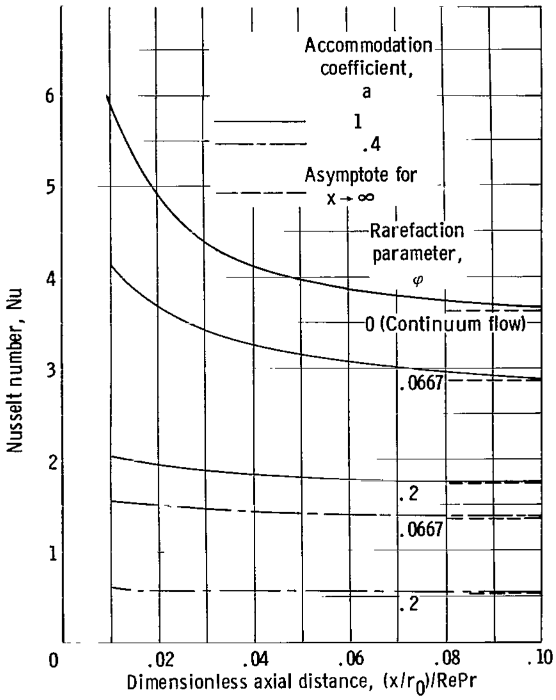

Figure 11. - Variation of local Nusselt number along tube for uniform wall temperature. Specular reflection coefficient, 1; ratio of specific heats, 1.4; Prandtl number, 0.73.

Uniform Wall Heat Flux (Ref. 3)

The longitudinal variation of the bulk temperature, the temperature of the gas adjacent to the wall, and the wall temperature corresponding to a uniform heat flux along the duct length is sketched in figure 12(a). With gas rarefaction, the wall temperature t_w, at a given axial location, is increased above the corresponding continuum-flow value. Then the wall-to-bulk temperature difference for slip flow $(t_w - t_b)_{sf}$ is greater than the corresponding difference for continuum flow $(t_w - t_b)_{cf}$. Since the Nusselt modulus Nu is inversely proportional to $t_w - t_b$, it is clear that $(Nu)_{sf} \leq (Nu)_{cf}$. Hence, the gas rarefaction reduces the Nusselt modulus below its continuum value at all positions along the duct.

Uniform Wall Temperature

Figure 12(b) illustrates the longitudinal variation of wall, contiguous gas, and bulk temperatures along a duct as the result of a step change in wall temperature. In the absence of gas rarefaction, the gas adjacent to the wall assumes the wall temperature. With gas rarefaction, t_g is always less than t_w along the duct length. In addition, the rarefaction decreases the bulk

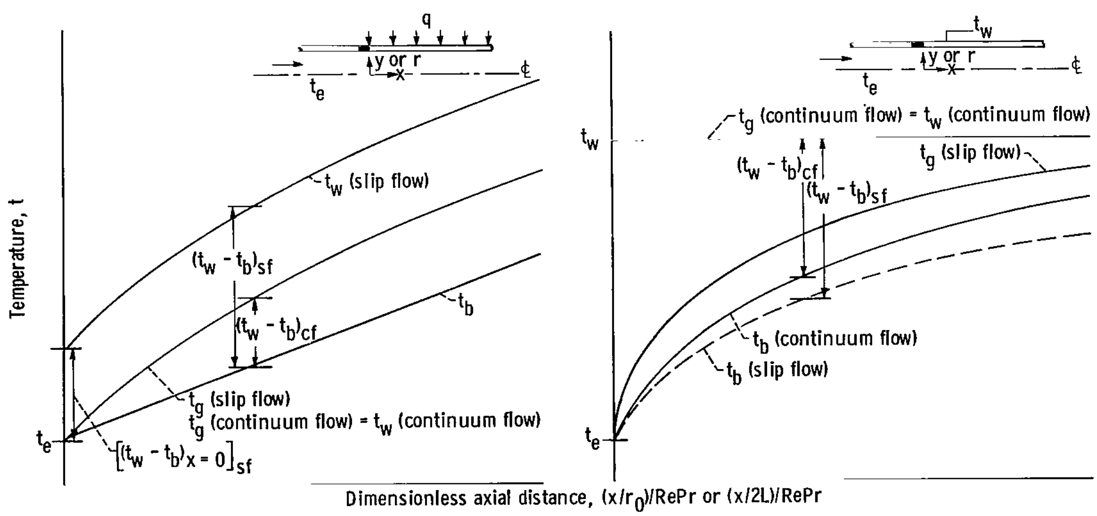

(a) Uniform wall heat flux.

(b) Uniform wall temperature.

Figure 12. - Longitudinal variation of temperatures.

temperature below its continuum value at all axial locations along the duct. Then, since t_w is constant along the duct length, it is apparent that, as in the uniform wall heat-flux case, $(t_w - t_b)_{sf}$ is greater than $(t_w - t_b)_{cf}$, and hence $(Nu)_{sf} \leq (Nu)_{cf}$. Consequently, for both uniform wall heat flux and uniform wall temperature, the Nusselt numbers for slip flow are lower than those for continuum flow.

CONCLUDING REMARKS

An analysis has been carried out to study laminar, forced-convection heat transfer to a slightly rarefied gas flowing between parallel plates or in a circular tube with the conduit walls kept at constant temperature. The wall heat-flux requirement and the Nusselt number in both the entrance and fully developed regions can be obtained as functions of the mean free path. Asymptotic solutions supplying accurate knowledge of the higher eigenvalues and important constants are presented. Results are presented graphically, and, thus, the heat-flux requirements and Nusselt numbers for the conduits can be determined quickly and easily. A qualitative explanation of rarefaction effects in which the more important physical aspects of the problem are represented has been given.

There are a few final remarks that should be made with reference to the analyses. More complicated wall boundary conditions than those considered here could be treated. For example, the parallel-plate channel could be treated for the case of unequal wall temperatures. This would require the determination of an additional set of eigenvalues and constants, the so-called odd eigenconstants (refs. 11 and 12), such that the complete solution to the case of unequal wall temperature is obtained by superposing these odd quantities with the even eigenvalues and constants that have been determined in the present study, eigenconstants for the case $\sigma = 2$. At first glance, it might appear that the results for the present case $\sigma = 1$ could be also used to obtain the case of unequal wall temperatures. The adiabatic wall boundary condition $(\partial t/\partial y)_w = 0$ for the case $\sigma = 1$, however, produces an axial temperature variation along that wall, and hence the boundary conditions of constant, but unequal, wall temperatures would not be satisfied upon the use of the present case $\sigma = 1$. The results for the case of $\sigma = 1$ would be useful, of course, in the consideration of boundary conditions such as constant heat flux on one wall and constant temperature on the other (ref. 13). The analysis could also be carried out for other geometries such as the annulus.

Several other, less frequently considered, rarefaction effects have been cited in the literature. These are wall shear work (ref. 14), modified temperature jump (ref. 15), and thermal creep velocity (refs. 4 and 5). The modification due to each of these additional rarefaction effects of the fully developed heat-transfer characteristics for laminar flow in tubes has been considered in reference 1. None of these rarefaction effects have been considered in the present analyses. The first two slip effects can be incorporated in the present study without too much difficulty; the basic procedures are illustrated in reference 1 (for fully developed heat transfer). Further discussion would add little to what has been said in reference 1 concerning these effects.

Inclusion of the thermal creep velocity, however, would give rise to an extremely complicated mathematical problem, for then the temperature and velocity fields are mutually interdependent. For example, the slip-flow boundary conditions for the parallel-plate channel system (eqs. (2) and (3) or ref. 3) must be altered to read, respectively,

$$u_s = \pm\xi_u\left(\frac{\partial u}{\partial y}\right)_{y=\mp L} + \frac{3}{4}\,\frac{\mu R_g}{p}\left(\frac{\partial t}{\partial x}\right)_{y=\mp L} \qquad \text{for} \quad \sigma = 2$$

$$u_s = \pm\xi_u\left(\frac{\partial u}{\partial y}\right)_{y=\left|\begin{smallmatrix}0\\2L\end{smallmatrix}\right.} + \frac{3}{4}\,\frac{\mu R_g}{p}\left(\frac{\partial t}{\partial x}\right)_{y=\left|\begin{smallmatrix}0\\2L\end{smallmatrix}\right.} \qquad \text{for} \quad \sigma = 1$$

The second term on the right side of each of these equations represents the thermal creep effect.

The thermal creep velocity effect would be expected to moderate the results given here. A more precise study that would account for the thermal creep velocity is certainly well in order. The results given here represent the special case when the thermal creep velocity is negligible. From these results, however, it has been possible to provide a physical interpretation of the rarefaction effects for different thermal-boundary conditions. In addition, from the results the design engineer can make a rapid, reasonably accurate estimation of slight rarefaction effects on heat transfer to gases flowing in conduits.

Lewis Research Center
National Aeronautics and Space Administration
Cleveland, Ohio, August 25, 1964

APPENDIX A

SYMBOLS

A	integration constant, $[f(0)]^{1/4}/2$
a	accommodation coefficient
B	integration constant, $[f(0)]^{1/4}/2$
B_n	coefficient defined by eq. (38)
b_n	coefficient in series expansion for parallel-plate channel
C_m	coefficient defined by eq. (72)
c_m	coefficient in series expansion for circular tube
c_p	specific heat of gas
D_H	hydraulic diameter for parallel-plate channel, 4L
D_T	thermal diameter for parallel-plate channel, $8L/\sigma$
d	tube diameter, $2r_0$
E	constant defined by eq. (34)
F	constant defined by eq. (46)
$f(\eta)$	dimensionless velocity for parallel-plate channel, $u(\eta)/\overline{u}$
$f(\omega)$	dimensionless velocity for circular tube, $u(\omega)/\overline{u}$
g	specular reflection coefficient
h	heat-transfer coefficient, $q/(t_w - t_b)$
I	indefinite integral defined by eq. (29)
I_1	definite integral defined by eq. (33)
J	indefinite integral defined by eq. (41)
J_1	definite integral defined by eq. (45); $J_1 = I_1$
K_1	definite integral defined by eq. (67)
L	half-distance between plates
l	mean free path

M	constant defined by eqs. (69)
N	constant defined by eqs. (69)
Nu	Nusselt number, hD_T/κ for parallel-plate channel, hd/κ for circular tube
Pr	Prandtl number, $\mu c_p/\kappa$
p	gas pressure
q	rate of heat transfer per unit area from wall to gas
R	radial distribution function for circular tube
R_g	gas constant
R_m	eigenfunctions of eqs. (57)
$R'(1)$	slope of $R(\omega)$ at tube wall
Re	Reynolds number, $2\rho\bar{u}L/\mu$ for parallel-plate channel, $\rho\bar{u}d/\mu$ for circular tube
r	radial coordinate
r_0	tube radius
T	dimensionless temperature difference, $(t - t_w)/(t_e - t_w)$
t	gas temperature
t_g	temperature of gas adjacent to wall
u	gas velocity
X	axial distribution function
x	axial coordinate
Y	transverse distribution function for parallel-plate channel
Y_n	eigenfunctions of eqs. (11)
$Y'(1)$	slope of $Y(\eta)$ at heated wall
y	transverse coordinate
α	thermal diffusivity, $\kappa/\rho c_p$
β_m	eigenvalues of eqs. (57)

β_n eigenvalues of eqs. (11)

Γ dimensionless temperature-jump coefficient, $\xi_t/2L$

γ ratio of specific heats

δ_n $\sqrt{\beta_n}\, I_1$

ϵ_n $\sqrt{\beta_n}\, J_1$

ζ dimensionless axial distance for parallel-plate channel, $\sigma^2(x/2L)/RePr$

η dimensionless coordinate, $\sigma y/2L$

θ dimensionless velocity slip coefficient, ξ_u/d

κ gas thermal conductivity

λ dimensionless velocity slip coefficient, $\xi_u/2L$

μ viscosity of gas

ξ_t temperature-jump coefficient

ξ_u velocity-slip coefficient

ρ gas density

σ symmetry number

τ_m $\sqrt{\beta_m}\, K_1$

φ rarefaction parameter, $\mu\sqrt{R_g t}/2pL$ for parallel-plate channel, $\mu\sqrt{R_g t}/pd$ for circular tube

ψ dimensionless axial distance for circular tube, $4(x/r_0)/RePr$

ω dimensionless coordinate, r/r_0

Subscripts:

b bulk condition of gas

c centerline

cf continuum flow

d fully developed region

e entrance, $x = 0$

s slip

sf slip flow

w condition at wall

0 continuum-flow condition

Superscript:

$(\bar{\ })$ average value

APPENDIX B

EVALUATION OF SERIES COEFFICIENTS b_n

The coefficients of the series expansion (eq. (10)) are determined as the quotient of two integrals (eq. (13)):

$$b_n = \frac{\int_0^1 f(\eta)Y_n(\eta)d\eta}{\int_0^1 f(\eta)Y_n^2(\eta)d\eta} \tag{B1}$$

With the use of equation (11a), the integral appearing in the numerator may be written as

$$\int_0^1 f(\eta)Y_n(\eta)d\eta = -\frac{1}{\beta_n}\int_0^1 \frac{d^2Y_n}{d\eta^2}\,d\eta = -\frac{1}{\beta_n}\left(\frac{dY_n}{d\eta}\right)\Bigg|_0^1 = -\frac{1}{\beta_n}\left(\frac{dY_n}{d\eta}\right)_{\eta=1} \qquad \text{for} \quad \sigma = 2,1 \tag{B2}$$

since $(dY_n/d\eta)_{\eta=0} = 0$.

To evaluate the integral in the denominator of equation (B1), let Y_ν and Y_n be the solutions associated with two distinct values of β, β_ν, and β_n. This means that

$$\frac{d^2Y_\nu}{d\eta^2} + \beta_\nu f(\eta)Y_\nu = 0$$

and

$$\frac{d^2Y_n}{d\eta^2} + \beta_n f(\eta)Y_n = 0$$

The first equation is multiplied by Y_n and the second by Y_ν, and then the second equation is subtracted from the first. The result, after transposing, is

$$(\beta_n - \beta_\nu)Y_\nu Y_n f(\eta) = -\frac{d}{d\eta}\left(Y_\nu \frac{dY_n}{d\eta} - Y_n \frac{dY_\nu}{d\eta}\right)$$

If this is integrated between 0 and 1, the following is obtained:

$$(\beta_n - \beta_\nu) \int_0^1 Y_\nu Y_n f(\eta) d\eta = - \left(Y_\nu \frac{dY_n}{d\eta} - Y_n \frac{dY_\nu}{d\eta} \right) \Bigg|_0^1 \tag{B3}$$

where $Y_\nu(\eta,\beta_\nu)$ and $Y_n(\eta,\beta_n)$ for $\nu \neq n$ are orthogonal functions with respect to the weight function $f(\eta)$; that is,

$$\int_0^1 Y_\nu Y_n f(\eta) d\eta = 0 \qquad \text{for} \quad \nu \neq n \tag{B4}$$

This property of the eigenfunctions was used in obtaining equation (B1).

If $\beta_\nu = \beta_n$, the integral on the left side of equation (B3) becomes the integral of the square of the characteristic function:

$$\int_0^1 Y_n^2 f(\eta) d\eta = - \lim_{\nu \to n} \frac{\left(Y_\nu \dfrac{dY_n}{d\eta} - Y_n \dfrac{dY_\nu}{d\eta} \right) \Bigg|_0^1}{\beta_n - \beta_\nu}$$

The expression on the right assumes the indeterminate form 0/0. Hence, it is necessary to apply l'Hospital's rule and differentiate numerator and denominator with respect to β_ν before setting $\beta_\nu = \beta_n$. Carrying out this differentiation results in

$$\int_0^1 f(\eta) Y_n^2(\eta) d\eta = \left(\frac{\partial Y_n}{\partial \beta_n} \frac{\partial Y_n}{\partial \eta} - Y_n \frac{\partial^2 Y_n}{\partial \beta_n \, \partial \eta} \right) \Bigg|_0^1 = \left(\frac{\partial Y_n}{\partial \eta} \frac{\partial Y_n}{\partial \beta_n} \right)_{\eta=1}$$

$$- \left(Y_n \frac{\partial^2 Y_n}{\partial \beta_n \, \partial \eta} \right)_{\eta=1} + \left(Y_n \frac{\partial^2 Y_n}{\partial \beta_n \, \partial \eta} \right)_{\eta=0} \tag{B5}$$

Near $\eta \sim 0$, the normalization convention $Y_n(0) \equiv 1$ as well as the boundary condition $dY_n/d\eta = 0$ at $\eta = 0$ require that the solution to equation (11) be given by $Y_n(\eta \sim 0) = \cos(\sqrt{\beta_n f(0)}\, \eta)$. Hence, at $\eta = 0$,

$$Y_n(0) \equiv 1$$

and

$$\left(\frac{\partial^2 Y_n}{\partial \beta_n \, \partial \eta}\right) = 0$$

Thus, equation (B5) reduces to

$$\int_0^1 f(\eta) Y_n^2 \, d\eta = \left(\frac{\partial Y_n}{\partial \eta} \frac{\partial Y_n}{\partial \beta_n} - Y_n \frac{\partial^2 Y_n}{\partial \beta_n \, \partial \eta}\right)_{\eta=1} \tag{B6}$$

Into this expression, there is now substituted the boundary condition

$$Y_n(1) = -\sigma \frac{\xi_t}{2L} \left(\frac{dY_n}{d\eta}\right)_{\eta=1}$$

This gives

$$\int_0^1 f(\eta) Y_n^2(\eta) d\eta = \left(\frac{\partial Y}{\partial \beta} + \sigma \frac{\xi_t}{2L} \frac{\partial^2 Y}{\partial \beta \, \partial \eta}\right)_{\substack{\eta=1 \\ \beta=\beta_n}} \left(\frac{\partial Y_n}{\partial \eta}\right)_{\eta=1} \tag{B7}$$

Therefore

$$b_n = -\frac{1}{\beta_n \left(\frac{\partial Y}{\partial \beta} + \sigma \frac{\xi_t}{2L} \frac{\partial^2 Y}{\partial \beta \, \partial \eta}\right)_{\substack{\eta=1 \\ \beta=\beta_n}}} \tag{B8}$$

If $\xi_t/2L = 0$, that is, if the boundary condition at $\eta = 1$ is of the simpler form

$$Y_n(1) = 0$$

the correct solution is obtained by setting $Y_n(1) = 0$ in equation (B6). This gives

$$\int_0^1 f(\eta) Y_n^2(\eta) d\eta = \left(\frac{\partial Y}{\partial \beta} \frac{\partial Y}{\partial \eta}\right)_{\substack{\eta=1 \\ \beta=\beta_n}} \qquad \text{for} \quad \frac{\xi_t}{2L} = 0 \tag{B9}$$

Therefore

$$b_n = - \frac{1}{\left(\beta \dfrac{\partial Y}{\partial \beta}\right)_{\substack{\eta=1 \\ \beta=\beta_n}}} \qquad \text{for} \quad \frac{\xi_t}{2L} = 0 \tag{B10}$$

This result resembles the equation for the continuum-flow coefficients (ref. 7).

REFERENCES

1. Sparrow, E. M., and Lin, S. H.: Laminar Heat Transfer in Tubes Under Slip-flow Conditions. Jour. Heat Transfer (Trans. ASME), ser. C, vol. 84, no. 4, Nov. 1962, pp. 363-369.

2. Deissler, R. G.: An Analysis of Second-Order Slip Flow and Temperature-jump Boundary Conditions for Rarefied Gases. Int. Jour. Heat and Mass Transfer, vol. 7, no. 6, June 1964, pp. 681-694.

3. Inman, R. M.: Laminar Slip Flow Heat Transfer in a Parallel-Plate Channel or a Round Tube With Uniform Wall Heating. NASA TN D-2393, 1964.

4. Kennard, E. H.: Kinetic Theory of Gases. McGraw-Hill Book Co., Inc., 1938, p. 291.

5. Schaaf, S. A., and Chambre, P. L.: Flow of Rarefied Gases. Princeton Univ. Press, 1961, p. 34.

6. Dzung, L. S.: Heat Transfer in a Flat Duct with Sinusoidal Heat Flux Distribution. Proc. Second U.N. Conf. on Peaceful Uses of Atomic Energy (Geneva), vol. 7, 1958, pp. 671-675.

7. Sellars, J. R., Tribus, M., and Klein, J. S.: Heat Transfer to Laminar Flow in a Round Tube or Flat Conduit - The Graetz Problem Extended. Trans. ASME, vol. 78, no. 2, Feb. 1956, pp. 441-448.

8. Merzbacher, E.: Quantum Mechanics. John Wiley & Sons, Inc., 1961, p. 112.

9. Carslaw, H. S., and Jaeger, J. C.: Conduction of Heat in Solids. Oxford Univ. Press, 1959, p. 491.

10. Dzung, L. S.: Heat Transfer in a Round Duct with Sinusoidal Heat Flux Distribution. Proc. Second U.N. Conf. on Peaceful Uses of Atomic Energy (Geneva), vol. 7, 1958, pp. 657-670.

11. Cess, R. D., and Shaffer, E. C.: Summary of Laminar Heat Transfer Between Parallel Plates with Unsymmetrical Wall Temperatures. Jour. Aero/Space Sci., vol. 26, no. 8, Aug. 1959, p. 538.

12. Hatton, A. P., and Turton, J. S.: Heat Transfer in the Thermal Entry Length With Laminar Flow Between Parallel Walls at Unequal Temperatures. Int. Jour. Heat and Mass Transfer, vol. 5, 1962, pp. 673-679.

13. Lundberg, R. E., Reynolds, W. C., and Kays, W. M.: Heat Transfer with Laminar Flow in Concentric Annuli with Constant and Variable Wall Temperature with Heat Flux. NASA TN D-1972, 1963.

14. Maslen, Stephen H.: On Heat Transfer in Slip Flow. Jour. Aero. Sci., vol. 25, no. 6, June 1958, pp. 400-401.

15. Oman, Richard A., and Scheuing, Richard A.: On Slip-Flow Heat Transfer to a Flat Plate. Jour. Aero. Sci., vol. 26, no. 2, Feb. 1959, pp. 126-127.

NASA-Langley, 1964 E-2667

2/7/05

"The aeronautical and space activities of the United States shall be conducted so as to contribute . . . to the expansion of human knowledge of phenomena in the atmosphere and space. The Administration shall provide for the widest practicable and appropriate dissemination of information concerning its activities and the results thereof."

—NATIONAL AERONAUTICS AND SPACE ACT OF 1958

NASA SCIENTIFIC AND TECHNICAL PUBLICATIONS

TECHNICAL REPORTS: Scientific and technical information considered important, complete, and a lasting contribution to existing knowledge.

TECHNICAL NOTES: Information less broad in scope but nevertheless of importance as a contribution to existing knowledge.

TECHNICAL MEMORANDUMS: Information receiving limited distribution because of preliminary data, security classification, or other reasons.

CONTRACTOR REPORTS: Technical information generated in connection with a NASA contract or grant and released under NASA auspices.

TECHNICAL TRANSLATIONS: Information published in a foreign language considered to merit NASA distribution in English.

TECHNICAL REPRINTS: Information derived from NASA activities and initially published in the form of journal articles.

SPECIAL PUBLICATIONS: Information derived from or of value to NASA activities but not necessarily reporting the results of individual NASA-programmed scientific efforts. Publications include conference proceedings, monographs, data compilations, handbooks, sourcebooks, and special bibliographies.

Details on the availability of these publications may be obtained from:

SCIENTIFIC AND TECHNICAL INFORMATION DIVISION

NATIONAL AERONAUTICS AND SPACE ADMINISTRATION

Washington, D.C. 20546